Cytochrome c folding triggered by electron transfer

Gary A Mines, Torbjörn Pascher, Sonny C Lee, Jay R Winkler and Harry B Gray

Background: Experimental and theoretical studies of protein folding suggest that the free-energy change associated with the folding process is a primary factor in determining folding rates. We have recently developed a photochemical electron-transfer-triggering method to study protein-folding kinetics over a wide range of folding free energies. Here, we have used this technique to investigate the relationship between folding rate and free-energy change using cytochromes *c* from horse (h-cyt *c*) and yeast (y-cyt *c*), which have similar backbone folds but different amino-acid sequences and, consequently, distinct folding energies.

Results: The folding free energies for oxidized and reduced h-cyt *c* and y-cyt *c* are linear functions of the denaturant (guanidine hydrochloride) concentration, but the concentration required to unfold half of the protein is 1.5 M lower for y-cyt *c*. We measured the folding rates of reduced h-cyt *c* and y-cyt *c* over a range of guanidine hydrochloride concentrations at two temperatures. When driving forces are matched at the appropriate denaturant concentrations, the two homologs have comparable folding rates. The activation free energies for folding h-cyt *c* and y-cyt *c* are linearly dependent on the folding free energies. The slopes of these lines are similar (~0.4) for the two proteins, suggesting an early transition state along the folding reaction coordinate.

Conclusions: The free-energy relationships found for h-cyt *c* and y-cyt *c* folding kinetics imply that the height of the barrier to folding depends upon the relative stabilities of the unfolded and folded states. The striking correspondence in rate/free-energy profiles for h-cyt *c* and y-cyt *c* suggests that, despite low sequence homology, they follow similar folding pathways.

Address: Beckman Institute, California Institute of Technology, Pasadena, CA 91125 USA.

Correspondence: Jay R. Winkler and Harry B. Gray
e-mail: winkler@bilrc.caltech.edu
hbg@bilrc.caltech.edu

Key words: cytochrome *c*, electron transfer, protein folding

Received: **22 May 1996**
Revisions requested: **4 Jun 1996**
Revisions received: **7 Jun 1996**
Accepted: **11 Jun 1996**

Chemistry & Biology June 1996, **3**:491–497

Introduction

The complex process of protein folding involves dynamics on timescales that range from picoseconds to minutes [1–8]. We have developed a new method for initiating protein folding by electron-transfer chemistry that will permit measurements in the time range from nanoseconds to seconds [4]. Thermodynamic analyses suggest that many redox-active proteins will be amenable to this approach. Owing to the change in solvation, the formal potentials for redox cofactors in proteins are often shifted substantially from their potentials in aqueous solution [9,10]. A simple cycle can be drawn connecting an oxidized and reduced protein in both folded and unfolded configurations [9]. If the active-site reduction potentials are different for the folded and unfolded states ($\Delta E_f^\circ \equiv E_F^\circ - E_U^\circ$), then the free energies of folding the oxidized and reduced proteins will differ by a comparable amount ($\Delta(\Delta G_f^\circ) \equiv \Delta G_{f,OX}^\circ - \Delta G_{f,RED}^\circ$).

In aqueous solution, both the oxidized and reduced forms of redox proteins are usually folded, and ΔE°_f reflects the relative stabilities of the two forms. Addition of denaturants (e.g., urea or guanidine hydrochloride (GuHCl)) to protein solutions induces protein unfolding; the folding free energies under these conditions (ΔG_f) are often found to be linear functions of the denaturant concentration ([D], eq. 1).

$$\Delta G_f = \Delta G_f^o + m_D[D] \quad (1)$$

Indeed, linear extrapolation to infinite dilution of a plot of ΔG_f as a function of [D] is the most common method used to estimate ΔG_f° [11–13]. In redox proteins with large values of ΔE_f°, and similar values of $m_{D,OX}$ and $m_{D,RED}$, it will be possible to find denaturing conditions where one oxidation state of the protein is fully unfolded while the other is fully folded.

We have used cytochrome *c* in our studies of electron-transfer-initiated protein folding [4]. Cytochrome *c* is a small (12.5 kDa) protein in which the heme moiety is covalently bound to the peptide through thioether linkages with the Cys14 and Cys17 residues [14]. The imidazole Nϵ atom of His18 is bound at one axial heme site and is believed to remain coordinated to the iron atom except in strongly acidic solutions (pH ≤ 2.5) [15,16]. The sixth Fe ligand is the thioether sidechain of Met80; this ligand is not as tightly bound as His18, and is known

Figure 1

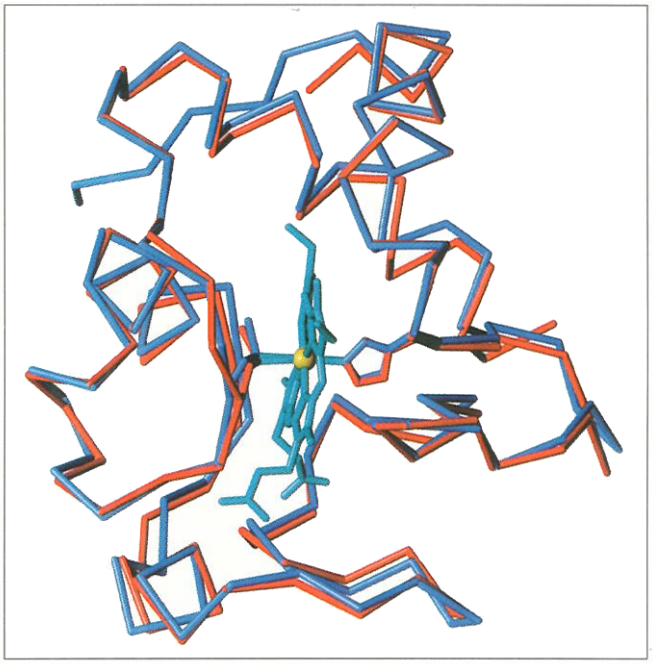

H-cyt *c* and y-cyt *c* have similar backbone structures. The backbone structures of h-cyt c^{III} (red [20]) and y-cyt c^{III} (blue [21]) are overlaid to maximize coincidence of heme atoms.

to dissociate under mild denaturing conditions [7]. The reduction potential of the heme in the folded protein (E°_{F}= 260 mV vs NHE (normal hydrogen electrode) [17]) is much higher than that of an exposed heme in aqueous solution (E°_{U}~ –100 mV [9,18]). This dramatic increase in potential upon protein folding indicates that reduced cytochrome *c* (cyt c^{II}) is more stable toward unfolding than the oxidized protein (cyt c^{III}).

Cytochromes *c* from over 100 species have been isolated and characterized [14,19]. Here, we compare the folding energetics and kinetics of two cytochromes *c*: horse (h-cyt *c*) and yeast (*Saccharomyces cerevisiae*, isoenzyme-1, Cys102→Ser mutant; y-cyt *c*). The amino-acid sequences of h-cyt *c* and y-cyt *c* are just 60 % identical [14]. Nevertheless, X-ray crystal structures show that the polypeptide backbones of the two proteins have similar folding patterns (Fig. 1) [20,21]. A consequence of the low sequence homology is that y-cyt *c* is more readily denatured than h-cyt *c*. However, when denaturant concentrations are adjusted to match the folding free energies for the two proteins, they have comparable folding rates.

Results and discussion

Folding energetics

We have probed the degree of folding in cyt *c* by monitoring the intensity of Trp59 fluorescence. The fluorescence is almost completely quenc folded protein, presumably via energy tran heme [22]. Unfolding the protein by additior produces an increase in fluorescence, ow greater separation between Trp59 and the GuHCl-induced unfolding of oxidized an h-cyt *c* and y-cyt *c* at 22.5 and 40 °C (pH described by simple two-state transitions, wh linear function of GuHCl concentration (Fig of $\Delta(\Delta G^{\circ}_{f})$ obtained by extrapolation to [GuH in good agreement with the difference in potentials of free hemes and of the hemes in proteins ($\Delta(\Delta G^{\circ}_{f})$ ~0.35 eV~–ΔE°_{f}).

The unfolding isotherms for h-cyt *c* and y-cyt that both oxidized and reduced forms of the y are ~15 kJ mol^{-1} less stable than the correspor of the horse protein. The y-cyt *c* unfolding ($[GuHCl]_{1/2}$) lie at GuHCl concentrations tha lower than those for h-cyt *c* (Table 1). A compa structures of the two proteins reveals that r

Figure 2

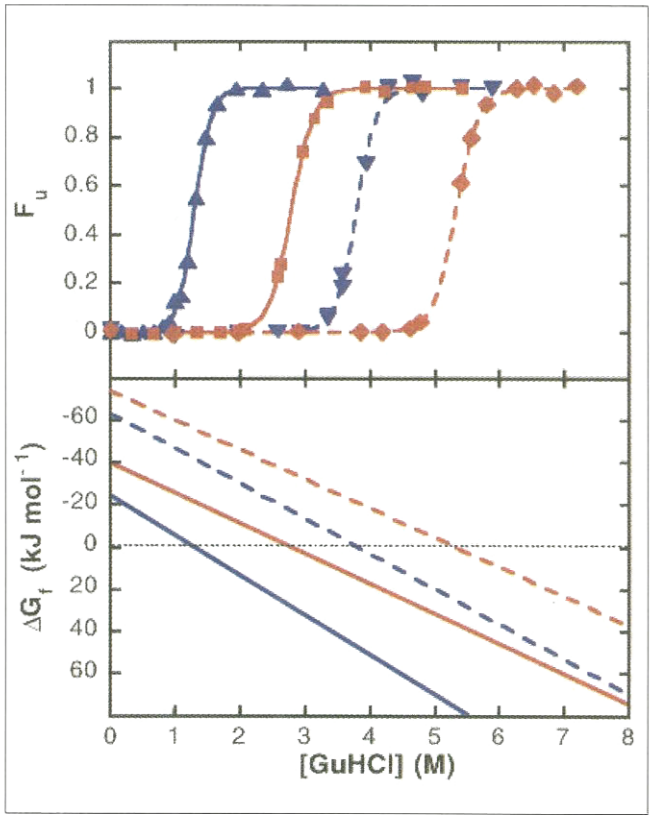

Both the oxidized and reduced forms of y-cyt *c* are ~15 kJ stable than the corresponding states of h-cyt *c*. Plots are s fraction of unfolded protein (F_u) as a function of GuHCl c (upper) and the corresponding unfolding isotherms (lower) (—) and reduced (- - -) h-cyt *c* (red) and y-cyt *c* (blue) at 2

sequence variability involves surface residues (Fig. 3). The residues in the inner core of the protein, which are probably responsible for determining the heme reduction potential, are highly conserved. Six distinct structural domains can be identified in cytochrome *c*: three α-helical regions (amino terminus (residues 1–13), carboxyl terminus (86-104), 60's helix (61–69)) and three omega loops (residues 20–35, 36–60, and 70–85) [20,21,23]. Of these six domains, only the 20–35 and 70–85 loops have highly conserved sequences (>80 %) in h-cyt *c* and y-cyt *c* [14]. The carboxy- and amino-terminal helices have particularly low sequence identity (37 % and 58 %, respectively). Presumably, the structures and solvation of all or part of these poorly conserved domains are responsible for the lower stability of the folded yeast protein.

Folding kinetics

For both h-cyt *c* and y-cyt *c*, we can define GuHCl concentration ranges in which >50 % of cyt c^{III} is unfolded and >90 % of cyt c^{II} is folded (h-cyt *c* (22.5 °C), 2.8–5.0 M; h-cyt *c* (40.0 °C), 2.4–4.3 M; y-cyt *c* (22.5 °C), 1.3–3.5 M; y-cyt *c* (40.0 °C), 0.8–2.9 M). Within these concentration ranges, rapid electron injection into unfolded cyt c^{III} initiates folding of the resultant cyt c^{II} [4]. Here, we will focus on slower folding events (>1 ms) that are associated with large changes in the ferroheme absorption spectrum. Folding on this timescale is initiated by electron injection into cyt c^{III} from a reductant (probably $CO_2^{\bullet-}$) generated in the UV laser photolysis of $Co(C_2O_4)_3^{3-}$ [4].

We have measured the folding kinetics of h-cyt c^{II} and y-cyt c^{II} at two temperatures (22.5, 40.0 °C, pH 7) over a wide range of GuHCl concentrations and thus over a wide range of folding free energies (ΔG_f = –10 to –40 kJ mol^{-1}). The observed kinetics are independent of protein concentration, but cannot in all cases be described by single-exponential functions. Adequate fits to the data can be obtained using biexponential decays or distributions of first-order decays. The latter model allows us to describe the observed kinetics in terms of a mean folding rate constant ($\overline{k}_f$) (see Materials and methods). Representative data, along with the best fits and residuals, are shown in Figure 4.

Values of $ln\ \overline{k}_f$ vary linearly with GuHCl concentration for both h-cyt *c* and y-cyt *c* (Fig. 5a); by analogy with equation 1, the activation free energy for folding ($\Delta G_f^{\ddagger}$) is a linear function of GuHCl concentration with slope $m_D^{\ddagger}$ (Table 1). In general, for a given temperature and GuHCl concentration, the measured or extrapolated mean folding rates for h-cyt *c* are more than one order of magnitude faster than those for y-cyt *c* . The linear dependence of ΔG_f on GuHCl concentration implies that $\Delta G_f^{\ddagger}$ also is a linear function of the folding free energy (with a slope of $m_D^{\ddagger}/m_D$). When the mean folding rates are plotted against ΔG_f, we find that the lines for h-cyt *c* and y-cyt *c* at a single temperature are close together (Fig. 5b). This remarkable observation strongly suggests that the height of the barrier for this folding step in cyt c^{II} depends only on the relative stabilities of the initial and final states. Theoretical studies have suggested that the folding free energy is a primary factor in determining folding rates [24,25]. The similar rate/free-energy dependences for these two cyt *c* homologs

Figure 3

H-cyt *c* and y-cyt *c* have different amino-acid sequences. The backbone structures of h-cyt *c* (left) and y-cyt *c* (right) are shown, with the sidechains of unconserved amino acids highlighted (h-cyt *c*, red; y-cyt *c*, blue). Listed below the structures are the amino-acid sequences for h-cyt *c* (upper) and y-cyt *c* (lower).

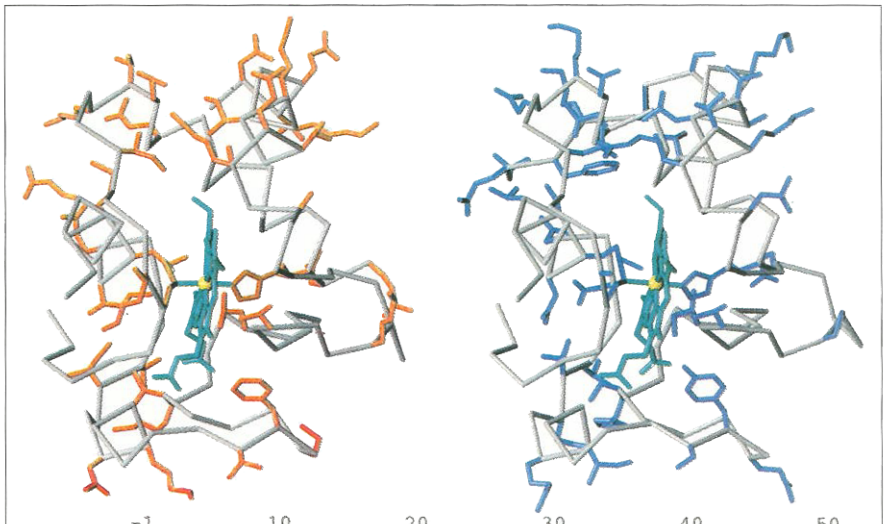

Figure 4

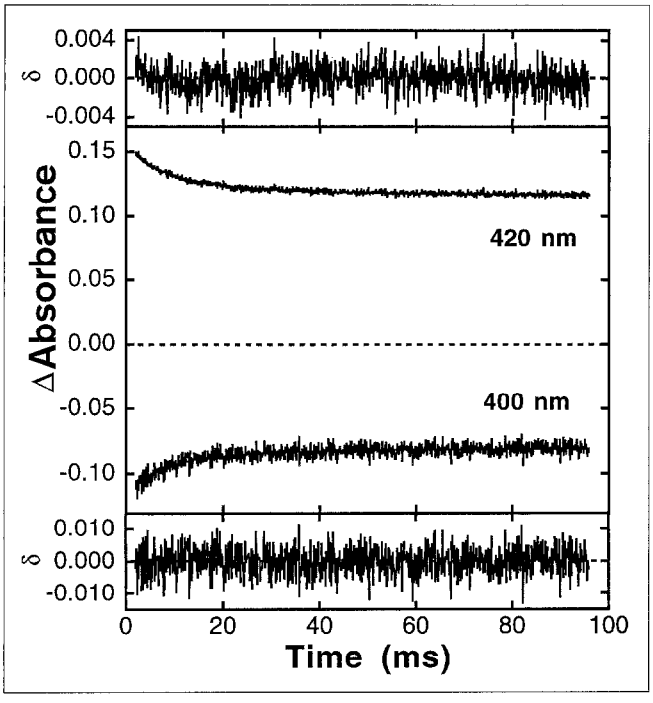

Folding kinetics of y-cyt c^{II} recorded at 420 and 400 nm (1 M GuHCl, pH 7, 40.0 °C). Residuals (δ) are shown for the best fits to a distribution of first-order decays.

provide compelling experimental support for this notion. Furthermore, the fact that the h-cyt *c* and y-cyt *c* $\overline{k_f}$ values have distinct dependences on GuHCl concentration indicates that this denaturant serves to shift the folding/unfolding equilibrium, but does not have a specific effect in determining the folding rate.

The Hammond postulate suggests that the slope of a linear plot of $\Delta G_f^{\ddagger}$ versus free energy ($m_D^{\ddagger}/m_D$) defines the location of the transition state along the reaction coordinate [26]. This analysis can be confounded by the presence of intermediates, and thus multiple transition states, along the cyt c^{II} folding pathway. In such a case, the significance of the $m_D^{\ddagger}/m_D$ ratio depends on the location of the intermediate(s) along the reaction coordinate, and on the dependence of the intermediate-state energy on the denaturant concentration. Recent studies, however, suggest that h-cyt c^{III} folding is a simple two-state process [27], and the same may be true for cyt c^{II}. Over the GuHCl concentration ranges used in these studies, we do not find significant deviations from a linear free-energy relationship. The slopes extracted from the $\Delta G_f^{\ddagger}$ versus free-energy plots for cyt c^{II} folding are all near 0.4 (Table 1), indicating a relatively early transition state along the folding reaction coordinate. This value of the $m_D^{\ddagger}/m_D$ ratio for cyt c^{II} folding is close to the value of 0.45 reported for h-cyt c^{III} [27], implying that the location of the transition state does on heme oxidation level. The striking corresp the rate/free-energy profiles for h-cyt *c* a suggests that, despite low sequence homolo proteins follow similar folding pathways and of the transition state is relatively insensi composition of the amino-acid sidechains in conserved regions.

Fersht and coworkers have used protein eng their extensive studies of folding and unfold barnase and chymotrypsin inhibitor [28–3 mutant protein, the parameter $\Phi_F = (\Delta\Delta$ ($\Delta\Delta G_f^{\ddagger}$ is the difference in activation free folding between the mutant and wild-typ $\Delta\Delta G_f$ is the difference in folding free ener

Figure 5

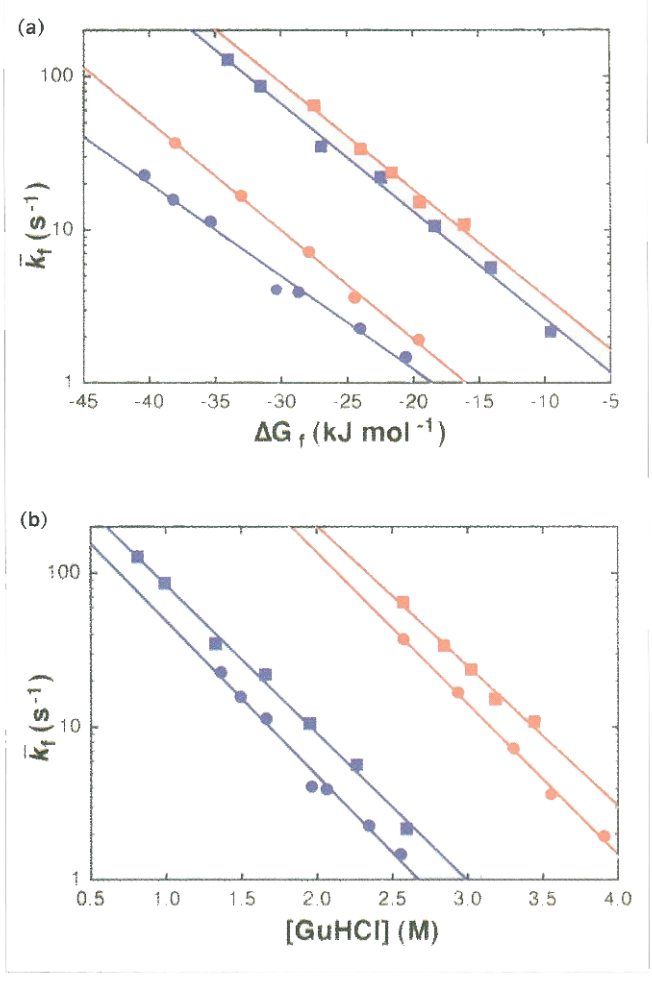

H-cyt *c* folds more than one order of magnitude faster tha given GuHCl concentration, but the folding rates of the t are similar for a given free-energy change. The rates of h- and y-cyt c^{II} (blue) folding at 22.5 (●) and 40 (■) °C (pH as functions of **(a)** GuHCl concentration and **(b)** ΔG_f.

Table I

Thermodynamic and kinetic parameters for h-cyt *c* and y-cyt *c* folding and unfolding (pH 7).

Protein	T (°C)	$[GuHCl]_{1/2}$ (M)	$-\Delta G_f^\circ$ (kJ mol^{-1})	m_D (kJ mol^{-1} M^{-1})	$m_D^\ddagger$ (kJ mol^{-1} M^{-1})	$m_D^\ddagger/m_D$
h-cyt c^{III}	22.5(5)	2.8(1)	40(1)	14.3(4)		
h-cyt c^{II}	22.5(5)	5.3(1)	74(3)	13.8(4)	5.6(5)	0.40
h-cyt c^{III}	40.0(5)	2.4(1)	30(1)	12.2(4)		
h-cyt c^{II}	40.0(5)	4.7(1)	61(10)	13.1(20)	5. 5(5)	0.42
y-cyt c^{III}	22.5(5)	1.3(1)	24(1)	18.9(5)		
y-cyt c^{II}	22.5(5)	3.8(1)	63(4)	16.6(10)	5.7(5)	0.34
y-cyt c^{III}	40.0(5)	0.8(1)	14(1)	17.1(1)		
y-cyt c^{II}	40.0(5)	3.3(1)	45(3)	13.7(8)	5.8(5)	0.42

Numbers in parentheses are estimated uncertainties.

the extent to which the residue(s) involved in the mutation form(s) native structure in the transition state ($\Phi_F = 0$ indicates an unfolded environment for the mutant residue(s); $\Phi_F = 1$ corresponds to a native environment) [29]. A critical caveat in this analysis is that it can be applied rigorously only to processes in which there is a single transition state. Nevertheless, if we consider y-cyt *c* to be a mutant of h-cyt *c*, then across the 1–3 M GuHCl concentration range (at 22.5 and 40.0 °C), we find that $\Phi_F \approx 0.5$. This value suggests that, for the poorly conserved regions of h-cyt *c* and y-cyt *c*, there is partial formation of native structure in the transition state for folding. Previous studies of h-cyt c^{III} folding are consistent with early development of native structure in the carboxy-terminal and amino-terminal helices [23,27,32], and these are two regions that have low sequence homology in the horse and yeast proteins. The value of $\Phi_F \approx 0.5$ that we find for h-cyt *c* and y-cyt *c* is thus consistent with the early formation of secondary structure in the terminal helices.

The variation in the folding rate with temperature can also be inferred from Figure 5. Although we have data at just two temperatures (22.5, 40.0 °C), it is clear that $\overline{k_f}$ increases as the temperature is raised. For folding rates at a fixed GuHCl concentration, the temperature variation is modest because of the reduction in folding driving force that accompanies the temperature increase. At fixed ΔG_f, however, folding rates increase by an order of magnitude between 22.5 and 40.0 °C. Theoretical studies of lattice models suggest that two competing effects lead to the observed temperature dependence of protein folding [33]. In the lattice models, both the internal energy and entropy decrease almost monotonically along the reaction coordinate. Within a limited temperature range, these two terms lead to a barrier in the free-energy profile for the reaction. The height of this barrier decreases with decreasing temperature, suggesting anomalous rate/temperature behavior. However, the dynamics of the diffusive motion required to reach the transition state will exhibit a normal temperature dependence and should determine the behavior at lower temperatures [33]. These theoretical predictions are generally consistent with our limited data set for h-cyt *c* and y-cyt *c*. The lattice models, however, do not explicitly account for stabilization of the unfolded protein by the denaturant. The denaturant could affect both the internal energy and entropy profiles along the reaction coordinate for cyt c^{II} folding, raising the possibility that there is a significant activation enthalpy for the reaction.

Significance

Comparisons of the folding energetics and kinetics of homologous proteins can provide important insights into folding pathways. Our investigations of h-cyt c^{II} and y-cyt c^{II} strongly suggest that the folding free energy is a primary factor in determining folding rates. These two proteins, with just 60 % identity in amino-acid sequence but very similar backbone structures, fold at nearly the same rate when their folding free-energy changes are equal. The differences in the h-cyt *c* and y-cyt *c* primary structures affect the position of the folding/unfolding equilibrium, but do not appear to modify the location of the transition state along the folding reaction coordinate. The value of $\Phi_F \approx 0.5$ associated with the change from h-cyt *c* to y-cyt *c* suggests that, on average, in the regions of the protein with low sequence homology, there is partial formation of native structure in the folding transition state. Transition-state analyses of this type, especially when coupled with protein engineering, can provide residue-specific information about folding pathways.

The diverse molecular motions involved in the conversion of a randomly configured polypeptide into a folded protein span more than twelve orders of magnitude in time. The power of electron-transfer-initiated protein folding is that it allows a direct examination of the events occurring in this entire time range; when coupled with protein engineering, this technique will

permit evaluation of the importance of individual residues in each step of the folding process.

Materials and methods

Type VI horse heart cytochrome *c* (Sigma) was used without further purification. Cys102→Ser *S. cerevisiae* cytochrome *c* was isolated and purified as described previously [34]. $K_3[Co(C_2O_4)_3]$ was prepared according to a published procedure [35]. Each guanidine hydrochloride (United States Biochemical, ultrapure grade) concentration was determined by measuring the refractive index of the solution [13].

Absorption spectra were measured using a Hewlett–Packard 8452 diode array spectrophotometer. Luminescence spectra were recorded using a Hitachi F-4500 spectrofluorimeter ($\lambda_{ex} = 292$ nm; $\lambda_{obsd} = 310–400$ nm). Unfolding isotherms for reduced cytochrome *c* were determined in the presence of excess sodium dithionite (200–400 μM). Fluorescence spectra were corrected for the effects of dithionite absorption at 292 nm. Transient absorption kinetics and spectra were measured using an apparatus described previously [36]. Samples for kinetics measurements were deoxygenated by repeated evacuation/fill cycles on a Schlenk line. Protein concentrations were typically 15 μM; $Co(C_2O_4)_3^{3-}$ concentrations were 32 μM; 100 mM sodium phosphate buffer, pH 7. Samples were excited with pulses from a XeCl excimer laser (308 nm, 5 mJ, 25 ns). Folding kinetics were monitored at 400 and 420 nm; the reported mean folding rates are the averages of the values obtained at the two wavelengths [4].

The observed folding kinetics could not always be described adequately by single-exponential functions, although good fits could be obtained with biexponential decays. Distributed kinetic models often are used in situations where there is a possibility of sample heterogeneity [37], as might be expected in protein folding. Therefore, folding kinetics were fit to a model that assumes a Gaussian distribution in the activation free energy for folding (eq. 2):

$$A(t) - A(\infty) \propto \int_{-\infty}^{\infty} \exp\{-kt\}\exp\{-[\alpha \ln(k/\bar{k})]^2\} d(\ln k) \quad (2)$$

where $A(t)$ is the transient absorption amplitude, $\bar{k}$ is the rate constant at the mean activation free energy, and α describes the width of the distribution. Data were fit using a hybrid version of the Levinberg–Marquadt nonlinear least-squares algorithm [38]. The widths of the distributions were relatively insensitive to GuHCl concentration and were somewhat broader at 40.0 °C than at 22.5 °C. It should be emphasized that both the biexponential and distributed functions afford good fits to the data. In most cases, we find that the rate constant for the dominant phase in the biexponential fits is within 50 % of the value of $\bar{k}$ obtained with the distributed model. Fitting alone cannot distinguish between the two models, and here we have elected to use values of $\bar{k}$. Values of $\bar{k}_f$ are obtained by multiplying $\bar{k}$ by the yield of formation of folded protein [4].

Acknowledgements

We thank J.N. Onuchic and P.G. Wolynes for helpful discussions. Our work is supported by the Swedish Natural Science Research Council (T.P.), the National Institutes of Health (G.A.M., 1 T32 GM08501), the National Science Foundation, and the Arnold and Mabel Beckman Foundation.

References

1. Phillips, C.M., Mizutani, Y. & Hochstrasser, R.M. (1995). Ultrafast thermally induced unfolding of RNase A. *Proc. Natl. Acad. Sci. USA* **92**, 7292–7296.
2. Williams, S., *et al.*, & Dyer, R.B. (1996). Fast events in protein folding: helix melting and formation in a small peptide. *Biochemistry* **35**, 691–697.
3. Jones, C.M., *et al.*, & Eaton, W.A. (1993). Fast events in initiated by nanosecond laser photolysis. *Proc. Natl. Aca* **90**, 11860–11864.
4. Pascher, T., Chesick, J.P., Winkler, J.R. & Gray, H.B. (19 folding triggered by electron transfer. *Science* **271**, 155
5. Nötling, B., Golbik, R. & Fersht, A.R. (1995). Submillisec protein folding. *Proc. Natl. Acad. Sci. USA* **92**, 10668–
6. Sosnick, T.R., Mayne, L., Hiller, R. & Englander, S.W. (19 barriers in protein folding. *Nat. Struct. Biol.* **1**, 149–156.
7. Elöve, G., Bhuyan, A.K. & Roder, H. (1994). Kinetic mecl cytochrome *c* folding: involvement of the heme and its lig *Biochemistry* **33**, 6925–6935.
8. Veeraraghavan, S., Rodriguez-Ghidarpour, S., MacKinnoı W.A., Pierce, M.M. & Nall, B.T. (1995). Prolyl isomerase stability of slow-folding intermediates. *Biochemistry* **34**, 12892–12902.
9. Bixler, J., Bakker, G. & McLendon, G. (1992). Electroche of protein folding. *J. Am. Chem. Soc.* **114**, 6938–6939.
10. Churg, A.K. & Warshel, A. (1986). Control of the redox p cytochrome *c* and microscopic dielectric effects in prote *Biochemistry* **25**, 1675–1681.
11. Yao, M. & Bolen, D.W. (1995). How valid are denaturant energy measurements? Level of confidence to common over an extended range of ribonuclease A stability. *Biocl* 3771–3781.
12. Linske-O'Connell, L.I., Sherman, F. & McLendon, G. (19 amino acid replacements at position 52 in yeast iso-1-cy *in vivo* and *in vitro* effects. *Biochemistry* **34**, 7094–710
13. Pace, N.C., Shirley, B.A. & Thomson, J.A. (1990). Measu conformational stability of a protein. In *Protein Structure: Approach.* (Creighton, T.F., ed.), pp. 311–330, IRL Press
14. Moore, G.R. & Pettigrew, G.W. (1990). *Cytochromes c: Structural, and Physicochemical Aspects.* Springer-Verla
15. Babul, J. & Stellwagen, E. (1972). Participation of the pr in the folding of cytochrome *c*. *Biochemistry* **11**, 1195–1
16. Drew, H.R. & Dickerson, R.E. (1978). The unfolding of cy in methanol and acid. *J. Mol. Biol.* **253**, 8420–8427.
17. Taniguchi, V.T., Sailasuta-Scott, N., Anson, F.C. & Gray, H Thermodynamics of metalloprotein electron transfer reac *Appl. Chem.* **52**, 2275–2281.
18. Santucci, R., Reinhard, H. & Brunori, M. (1988). Direct electrochemistry of the undecapeptide from cytochrome (microperoxidase) at a glassy carbon electrode. *J. Am.* C **110**, 8536–8537.
19. Scott, R.A. & Mauk, A.G. (1996). *Cytochrome c – A Mu Approach.* University Science Books, Sausalito, CA.
20. Bushnell, G.W., Louie, G.V. & Brayer, G.D. (1990). High- dimensional structure of horse heart cytochrome *c*. *J. Mc* 585–595.
21. Berghuis, A.M. & Brayer, G.D. (1992). Oxidation-state de conformational changes in cytochrome *c*. *J. Mol. Biol.* **22**
22. Tsong, T.Y. (1976). Ferricytochrome *c* chain folding meas energy transfer of tryptophan to the heme group. *Bioche* 5467–5473.
23. Bai, Y., Sosnick, T.R., Mayne, L. & Englander, S.W. (199 folding intermediates: native-state hydrogen exchange. S 192–197.
24. Bryngelson, J.D., Onuchic, J.N. & Wolynes, P.G. (1995). pathways and the energy landscape of protein folding – *Proteins: Struct. Func. Gen.* **21**, 167–195.
25. Onuchic, J.N., Wolynes, P.G., Luthey-Schulten, Z. & Soc (1995). Toward the outline of the topography of a realisti folding funnel. *Proc. Natl. Acad. Sci. USA* **92**, 3626–36
26. Hammond, G.S. (1955). A correlation of reaction rates. *Soc.* **77**, 334–338.
27. Sosnick, T.R., Mayne, L. & Englander, S.W. (1996). Mole collapse: the rate-limiting step in two-state cytochrome *c* *Proteins: Struct. Func. Gen.* **24**, 413–426.
28. Matouschek, A. & Fersht, A.R. (1993). Application of phy chemistry to engineered mutants of proteins: Hammond behavior in the transition state of protein folding. *Proc. N USA* **90**, 7814–7818.
29. Otzen, D.E., Itzhaki, L.S., El Masry, N.F., Jackson, S.E. & F (1994). Structure of the transition state for the folding/u barley chymostrypsin inhibitor 2 and its implications for n protein folding. *Proc. Natl. Acad. Sci. USA* **91**, 10422–1
30. Fersht, A.R., Itzhaki, L.S., El Masry, N.F., Matthews, J.M. &

(1994). Single versus parallel pathways of protein folding and fractional formation of structure in the transition state. *Proc. Natl. Acad. Sci. USA* **91**, 10426–10429.
31. Matouschek, A., Otzen, D.E., Itzhaki, L.S., Jackson, S.E. & Fersht, A.R. (1995). Movement of the position of the transition state in protein folding. *Biochemistry* **34**, 13656–13662.
32. Colón, W., Elöve, G.A., Wakem, L.P., Sherman, F. & Roder, H. (1996). Side-chain packing of the N- and C-terminal helices plays a critical role in the kinetics of cytochrome c folding. *Biochemistry* **35**, 5538–5549.
33. Socci, N.D., Onuchic, J.N. & Wolynes, P.G. (1996). Diffusive dynamics of the reaction coordinate for protein folding funnels. *J. Chem. Phys.* **104**, 5860–5868.
34. Mayo, S.L. (1988). Electron transfer in structurally engineered metalloproteins. Ph.D. thesis, California Institute of Technology.
35. Booth, H.S. (1939). *Inorganic Syntheses, Volume I.* McGraw-Hill Book Company, Inc., New York.
36. Stowell, M.H.B., Larsen, R.W., Winkler, J.R., Rees, D.C. & Chan, S.I. (1993). Transient electron-transfer studies on the two-subunit cytochrome c oxidase from *Paracoccus denitrificans*. *J. Phys. Chem.* **97**, 3054–3057.
37. Bright, F.V., Catena, G.C. & Huang, J. (1990). Evidence for lifetime distributions in cyclodextrin inclusion complexes. *J. Am. Chem. Soc.* **112**, 1343-1346.
38. Press, W.H., Flannery, B.P., Teukolsky, S.A. & Vetterling, W.T. (1989). *Numerical Recipes: The Art of Scientific Computing.* Cambridge University Press, New York.